QUARTERLY OF APPLIED MATHEMATICS
VOLUME XLIV, NUMBER 2
JULY 1986, PAGES 265–275

TRANSIENT DYNAMIC GREEN'S FUNCTIONS FOR A CRACKED PLANE*

BY

L. M. BROCK

University of Kentucky

Abstract. Closed-form solutions for the transient dynamic problems of a suddenly applied anti-plane concentrated force and concentrated impulse near a crack are obtained. The various wave signals comprising the solutions are identified, and their behavior noted. The concentrated force solution is then employed as a Green's function to solve the important problem of arbitrary screw dislocation motion near a crack edge.

1. Introduction. Problems of transient dynamic crack interaction with material boundaries, voids, inclusions or dislocations in linearly elastic solids arise in studies of seismology and fracture mechanics [1, 2]. These problems often defy analytic solution. However, as corresponding quasi-static and time-harmonic analyses [3] show, numerical treatments can be developed in terms of Green's function representations of the solutions. Because the crack edge singularity and traction-free crack surface conditions are automatically incorporated, such treatments can be made more efficient by using, instead of free-space Green's functions, Green's functions for a cracked space. However, these Green's functions must be available in analytically and computationally convenient forms, and their behavior well understood.

In this light, the related two-dimensional problem of a concentrated inplane force imposed suddenly near a semi-infinite crack was treated in [4]. Despite difficulties posed by the crack edge-force separation characteristic length, it was shown that the solution could be obtained in a relatively simple form. Nevertheless, multiple integration was involved, so that a thorough study of solution behavior was beyond the scope of the paper.

Therefore, to gain insight into the behavior, especially the wave propagation response, of Green's functions in a cracked plane, this article considers the related problems of a suddenly imposed concentrated anti-plane force and a concentrated anti-plane impulse. It will be seen that closed-form solutions can be obtained.

Then, to illustrate the aforementioned utility of a cracked plane Green's function, these solutions are used to solve the important problem of a screw dislocation moving with a nonuniform speed along an arbitrary path near a crack in an unbounded plane. The crack

* Received October 22, 1984.

edge stress field for this problem has been derived [5] by direct methods; the complete solution is obtained here in a few steps.

As in [4], the unbounded plane is isotropic, homogeneous and linearly elastic. The analysis begins in the next section with the formulation of the concentrated force problem. In subsequent sections, the problem solution is derived. The concentrated impulse problem then follows by inspection.

2. Concentrated force problem formulation. Consider the plane containing a crack defined in terms of the Cartesian coordinates (x, y) as $y = 0$, $x < 0$ and the polar coordinates (r, θ) as $\theta = \pm\pi$, where $r = \sqrt{x^2 + y^2}$, $\tan\theta = y/x(|\theta| \leqslant \pi)$. Prior to $\tau = \tau_0 > 0$, where $\tau =$ (rotational wave speed) $\times$(time), the plane is at rest. At $\tau = \tau_0$ a unit concentrated anti-plane force appears at the point $(x_0, y_0)(r_0, \theta_0)$. The force generates a cylindrical rotational wave which reaches the crack edge at $\tau = \tau_0 + r_0$. The resulting diffraction pattern is illustrated for $x_0 < 0, y_0 > 0$ in Fig. 1.

The governing equations for the problem are

$$\nabla^2 F - \ddot{F} + b_F = 0, \quad \frac{\partial F}{\partial y} = 0 \ (y = 0, x < 0), \quad F \equiv 0 \ (s < 0), \tag{2.1}$$

$$b_F = \delta(x - x_0)\delta(y - y_0)H(s), \qquad s = \tau - \tau_0 \tag{2.2}$$

where $F(x, y, x_0, y_0, s)$ is the anti-plane displacement, b_F represents the concentrated force, ∇^2 is the Laplacian, $(\cdot) \equiv \partial(\,)/\partial\tau$, δ and H are the Dirac and Heaviside functions. The characteristic length r_0 makes a direct solution of (2.1) by standard transform methods [6] difficult. Therefore, the problem is attacked by introducing the superposition

$$F = G + F_c, \tag{2.3}$$

$$\nabla^2 G - \ddot{G} + b_F = 0, \qquad G \equiv 0 \ (s < 0), \tag{2.4}$$

$$\nabla^2 F_c - \ddot{F}_c = 0, \quad \frac{\partial F_c}{\partial y} = -\frac{\partial G}{\partial y} \ (y = 0, x < 0), \quad F_c \equiv 0 \ (s < 0). \tag{2.5}$$

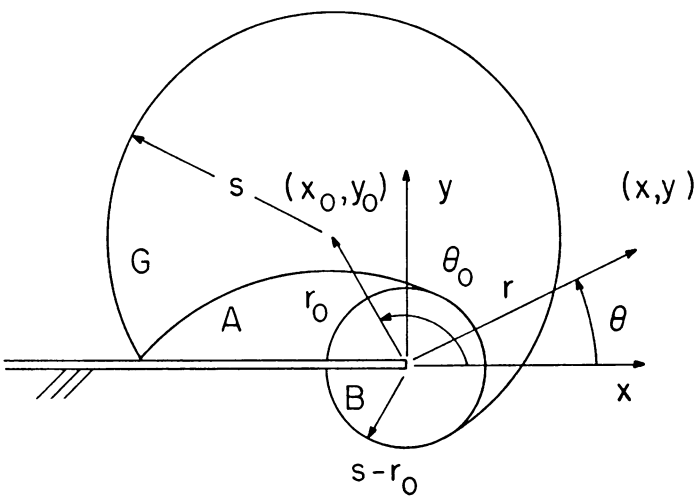

FIG. 1. Pattern of wavefronts for concentrated force.

Eqs. (2.4) are the governing relations for a concentrated force in an uncracked plane, while (2.5) define a displacement F_c generated by the imposition of a field $-\partial G/\partial y$ along a crack $y = 0, x < 0$. The solution to (2.4) is readily obtained [7] as

$$G = L\left(\frac{s}{R}\right), \quad L(u) = \frac{1}{2\pi}\ln\left[u + \sqrt{u^2 - 1}\right], \quad R = \sqrt{(x - x_0)^2 + (y - y_0)^2} \tag{2.6}$$

for $s \geqslant R$. Eq. (2.5) is attacked in the next section.

3. Solution for F_c. Equations of the form (2.5) have been treated [5, 8, 9] by recognizing that the general solution can be written as [7]

$$F_c(x, y, x) = \frac{1}{\pi}\iint_\Gamma T_F(p, q)\frac{dp\,dq}{\sqrt{(s - q)^2 - (x - p)^2 - y^2}},$$

$$T_F(x, s) = \frac{\partial F_c}{\partial y}(x, 0, s), \tag{3.1}$$

where Γ is the hyperbolic section of the space-time cone in the pq-plane defined by $s - q > \sqrt{(x - p)^2 + y^2}$, $0 \leqslant q < s$. Eqs. (2.4) and (2.5) specify T_F for $x < 0$. The results of [5] show that for $x > 0$

$$\pi T_F(x, s) = \frac{1}{\sqrt{v - u}}\int_K^v T_G(w, v)\frac{\sqrt{v - w}}{u - w}\,dw,$$

$$T_G(u, v) = \frac{\partial G}{\partial y}(x, 0, s) \tag{3.2}$$

when $s > r_0$ and vanishes otherwise. In (3.2)

$$\sqrt{2}\,v = s + x, \quad \sqrt{2}\,u = s - x, \quad \sqrt{2}\,K = \frac{r_0^2 + \sqrt{2}\,ux_0}{\sqrt{2}\,u + x_0} \tag{3.3}$$

where (u, v) are characteristic coordinates, w is an integration variable representing v-dependence and $v = K$ defines the intersection of the rotational wavefront generated by the concentrated force with the x-axis.

Differentiation of (2.6) and setting $y = 0$ yields

$$2\pi T_G = \frac{sy_0}{R_0^2\sqrt{s^2 - R_0^2}}, \quad R_0 = \sqrt{(x - x_0)^2 + y_0^2} \tag{3.4}$$

for $s > R_0$. Substitution of (3.4) into (3.2) in view of (3.3) gives the expression

$$2^{7/4}\pi^2 T_F(x, s) = \frac{y_0}{\sqrt{v - u}}\int_K^u \sqrt{\frac{u - w}{w - K}}\,\frac{w + u}{v - w}\,\frac{dw}{R_0^2} \tag{3.5}$$

for $x < 0$. The integrand of (3.5) has a branch cut $u < w < K$, and simple poles at $w = v > u$ and $w = u + \sqrt{2}(x_0 \pm i|y_0|)(R_0 = 0)$ which lie off the branch cut. Because the integrand behaves as $1/w$, $|w| \to \infty$, the integration can then be carried out by using the Cauchy residue theorem, and manipulation of the result yields

$$T_F = -T_G + \frac{1}{2\pi}\frac{1}{\sqrt{x}}\frac{y_0(r_0 + x)}{R_0^2\sqrt{r_0 + x_0}} \tag{3.6}$$

for $x > 0$, $s > r_0$. Eqs. (2.3) and (3.6) show that the normal derivative generated ahead of the crack edge is identical to that induced by the quasi-static application of the concentrated force.

4. Integral evaluation. With T_F known, F_c can be obtained from (3.1). In performing the evaluation, it is convenient to note that the integration areas in the pq-plane defined by Γ and T_F are of the two types illustrated in Fig. 2 for the case $x_0 > 0$. The characteristic coordinates (u, v) are used again, but now in terms of (p, q), so that the curve $v = M$ in Fig. 2 represents the Γ-defined hyperbola, $u = u^{\pm}(u^+ > u^-)$ denotes the intersection of the curves $v = K$, $v = M$ and $u = u_0$ denotes the intersection of the curves $v = M$, $v = u$. It is easily shown that

$$\sqrt{2}\,M = \frac{s^2 - r^2 - \sqrt{2}\,u(s + x)}{s - x - \sqrt{2}\,u}, \quad \sqrt{2}\,u_0 = s - r, \tag{4.1}$$

$$2\sqrt{2}\,(s + x - x_0)u^{\pm} = (s - x_0)^2 + y_0^2 - r^2 \pm \sqrt{s^2 - R^2}\,\sqrt{s^2 - \rho^2}, \tag{4.2}$$

$$\rho = \sqrt{(x - x_0)^2 + (y + y_0)^2}, \quad s + x - x_0 > 0. \tag{4.3}$$

For the case shown in Fig. 2a, the r.h.s. of (3.1) assumes, upon introducing the characteristic variables (u, v), the form A, where

$$4\pi^2 A = y_0 \int_{u^-}^{u^+} \frac{du}{\sqrt{s - x - \sqrt{2}\,u}\,\sqrt{x_0 + \sqrt{2}\,u}} \int_K^M \frac{u + v}{\sqrt{v - K}\,\sqrt{M - v}}\,\frac{dv}{R_0^2}. \tag{4.4}$$

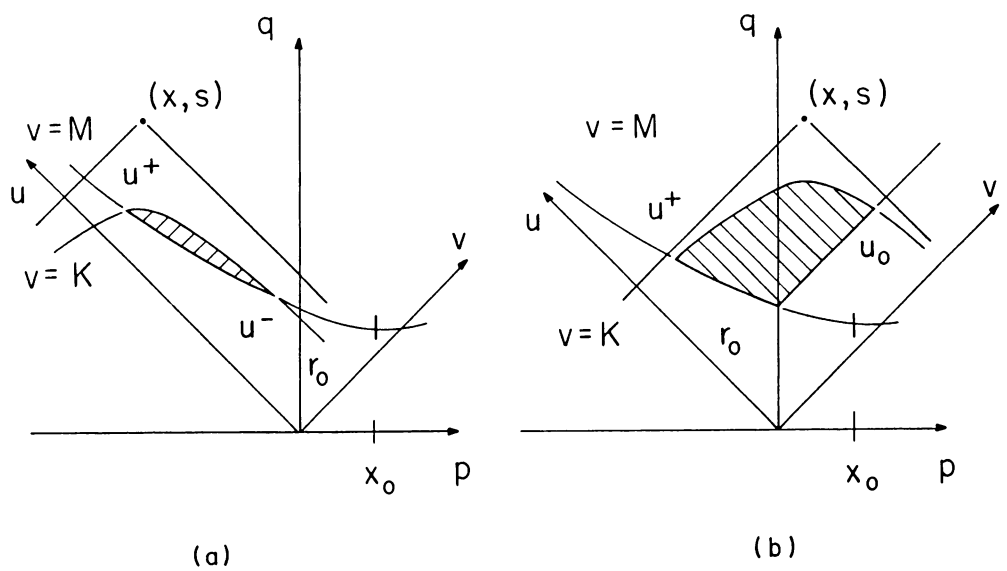

FIG. 2. Integration regions in pq-plane.

The v-integrand in (4.4) has a branch cut $K < v < M$, simple poles at $v = u + \sqrt{2}(x_0 + i|y_0|)(R_0 = 0)$, and behaves as $1/v$, $|v| \to \infty$. Therefore, the v-integration can be performed by using the Cauchy residue theorem to give

$$4\pi A = \frac{y_0}{2^{1/4}} \int_{u^-}^{u^+} \frac{\sqrt{U + u + \sqrt{2}x_0 - M}}{U\sqrt{s - x - \sqrt{2}u}\,(x_0 + \sqrt{2}u)}\,du, \quad U = \sqrt{(u + \sqrt{2}x_0 - M)^2 + 2y_0^2}. \tag{4.5}$$

A variable change and some manipulation then gives

$$4\pi A = y_0 \operatorname{Re} \int_{w^-}^{w^+} \frac{1}{W} \frac{dw}{s + x_0 - w}, \qquad W = \sqrt{y^2 + (x - X_0)^2 - (w - X_0)^2}, \tag{4.6}$$

where $w^{\pm} = s - \sqrt{2}u^{\pm}$, $X_0 = x_0 + i|y_0|$. A standard table [10] gives the indefinite integral of (4.6) which, upon substitution of $w^{\pm}$, evaluation of the real part and simplification in view of Figs. 1 and 2a, yields

$$A = k_r L\left(\frac{s}{R_+}\right), \qquad R_+ = \sqrt{(x - x_0)^2 + (|y| + |y_0|)^2} = \max(R, \rho) \tag{4.7}$$

where $R_+ < s < \Delta$ and

$$\Delta = r + r_0, \quad k_r = \operatorname{sgn}(yy_0)H(-xr_0 - x_0 r) \tag{4.8}$$

For the case shown in Fig. 2b, the r.h.s. of (3.1) can be rewritten as $B = B_1 + B_2$, where

$$4\pi^2 B_2 = \frac{y_0}{\sqrt{r_0 + x_0}} \int_{r_0/\sqrt{2}}^{u_0} \frac{du}{\sqrt{s - x - \sqrt{2}u}} \int_u^M \frac{\sqrt{2}r_0 + v - u}{\sqrt{v - u}\sqrt{M - v}} \frac{dv}{R_0^2}, \tag{4.9}$$

and B_1 differs from A only in that the lower u-integration limit is $r_0/\sqrt{2}$. By following the procedure for evaluation of A and comparing Figs. 1 and 2b, it is therefore easily shown that

$$2B_1 = L\left(\frac{s}{\rho}\right) - L\left(\frac{s}{R}\right) + L\left(\frac{\Delta}{R}\right) - L\left(\frac{\Delta}{\rho}\right) + 2k_r L\left(\frac{\Delta}{R_+}\right) \tag{4.10}$$

where $s > \Delta$ and it is noted that $\Delta \geqslant (R, \rho)$. The integrand in B_2 has a branch cut $u < v < M$, simple poles at $v = u + \sqrt{2}(x_0 + i|y_0|)$, and behaves as $1/v$, $|v| \to \infty$. Therefore, the Cauchy residue theorem can be applied to yield

$$4\pi B_2 = \frac{y_0}{2^{1/4}} \frac{1}{r_0 + x_0} \int_{r_0/\sqrt{2}}^{u_0} \frac{\sqrt{U + u + \sqrt{2}x_0 - M}}{U\sqrt{s - x - \sqrt{2}u}}\,du, \tag{4.11}$$

which, by the same manipulations applied to (4.5), gives

$$4\pi B_2 = \frac{y_0}{r_0 + x_0} \operatorname{Re} \int_r^{s - r_0} \frac{1}{W}\,dw. \tag{4.12}$$

The indefinite integral of (4.12) can be found [10] and, by then substituting the limits of integration, taking the real part, and performing some manipulations in view of Figs. 1 and 2b, we have

$$4\pi B_2 = \frac{y_0}{r_0 + x_0}\left[\Psi(s - r_0) - \Psi(r)\right], \quad \tan\Psi(w) = \frac{C\cos\Phi + h\sin\beta}{C\sin\Phi + h\cos\beta} \tag{4.13}$$

where $|\Psi| \leqslant \pi$, $s > \Delta$ and

$$C^2 = \sqrt{(r_+ r_-)^2 + h^4 - 2h^2 r_+ r_- \cos(\omega_- - \omega_+ - 2\beta)}, \qquad \tan\phi = \sqrt{\frac{C^2 - E^2}{C^2 + E^2}}, \tag{4.14}$$

$$h = \sqrt{(w - x_0)^2 + y_0^2}, \qquad \tan\beta = \frac{|y_0|}{w - x_0}, \tag{4.15}$$

$$r_\pm = \sqrt{(x - x_0)^2 + (y \pm |y_0|)^2}, \qquad \tan\omega_\pm = \frac{y \pm |y_0|}{x - x_0}. \tag{4.16}$$

Here $|\Phi, \beta, \omega_\pm| \leqslant \pi$ and

$$2(h^2 + E^2) = r_+^2 + r_-^2. \tag{4.17}$$

5. Concentrated force solution. The solution F can now be written as the sum of three signals A, B, and G:

$$F = AH(\Delta - s)H(s - R_+) + BH(s - \Delta) + GH(s - R). \tag{5.1}$$

Fig. 1 and the Heaviside function arguments in (5.1) show that G represents the cylindrical rotational wave radiated by the concentrated force, while the A-signal simultaneously represents the reflection of this wave from one side of the crack while cancelling it in the shadow zone on the opposite side. The B-signal represents the cylindrical rotational wave radiated from the crack edge upon arrival of the G-signal. The dependence of B_1 suggests that only the B_2-signal contains information about the singular nature of the crack edge field. Examination of (2.7), (4.7), (4.10), and (4.13) shows that the various signals are continuous at their respective wavefronts ($s = R$, $s = R_+$, $s = \Delta$).

More insight into the behavior of F can be gained by examining its spatial derivative. If, as indicated in Fig. 3, n is a coordinate directed at some angle ν w.r.t. the x-axis, then it is easily shown that

$$\frac{dF}{dn} = A_n H(\Delta - s)H(s - R_+) + B_n H(s - \Delta) + G_n H(s - R) \tag{5.2}$$

where $B_n = B_{1n} + B_{2n}$ and

$$A_n = -k_r P(s, R_+)\frac{dR_+}{dn}, \quad P(u, v) = \frac{1}{2}\frac{u}{v}\frac{1}{\sqrt{u^2 - v^2}}, \tag{5.3}$$

$$2B_{1n} = [P(s, R) - P(\Delta, R)]\frac{dR}{dn} + [P(\Delta, \rho) - P(s, \rho)]\frac{d\rho}{dn} + 2k_r \frac{R_+}{\Delta} P(\Delta, R_+)\left(\frac{dr}{dn} - \Delta\frac{dR_+}{dn}\right), \tag{5.4}$$

$$8\pi B_{2n} = -\frac{y_0}{r_0}\frac{1}{\sqrt{r_0 + x_0}\sqrt{r - x}}\frac{dr}{dn}$$

$$-\frac{y_0}{r_0 + x_0}\left[\frac{\cos(\omega_+ - \phi)}{r_+} + \frac{\cos(\phi - \omega_-)}{r_+}\right]\left[\frac{1}{2}\left(\frac{r}{r_0} - 1\right)\sqrt{\frac{r_0 + x_0}{r - x}} - \frac{h}{C}\cos(\beta + \Phi)\right]$$

$$-\frac{y_0}{r_0 + x_0}\left[\frac{\sin(\omega_+ - \phi)}{r_+} + \frac{\sin(\phi - \omega_-)}{r_-}\right]\left[\frac{1}{2}\left(\frac{r}{r_0} + 1\right)\sqrt{\frac{r_0 - x_0}{r - x}} - \frac{h}{C}\sin(\beta + \Phi)\right], \tag{5.5}$$

$$G_n = -P(s, R)\frac{dR}{dn} \tag{5.6}$$

and $(r_\pm, \omega_\pm, h, \Phi, C)$ are evaluated at $s - r_0$ in (5.5).

The distances (r, r_0, R, p) and angles (θ, θ_0, ν) are indicated in Fig. 3, as are the angles

$$\tan\Omega = \frac{y - y_0}{x - x_0}, \quad \tan\Omega_0 = \frac{-y_0}{x - x_0}, \quad \tan\Omega_+ = \operatorname{sgn}(y)\frac{|y| + |y_0|}{x - x_0}, \quad \tan\omega = \frac{y + y_0}{x - x_0} \tag{5.7}$$

where $|\Omega, \Omega_0, \Omega_+, \omega| \leqslant \pi$. Fig. 3 indicates that the derivatives in (5.3)–(5.6) can be written more compactly in terms of these angles:

$$\frac{dR}{dn} = \cos(\Omega - \nu), \quad \frac{dR_+}{dn} = \cos(\Omega_+ - \nu), \quad \frac{dr}{dn} = \cos(\theta - \nu), \quad \frac{d\rho}{dn} = \cos(\omega - \nu). \tag{5.8}$$

Examination of (5.2) in view of (5.3)–(5.8) shows that dF/dn is not continuous at its signal wavefronts, except perhaps for special combinations of (x, y, x_0, y_0, s, ν).

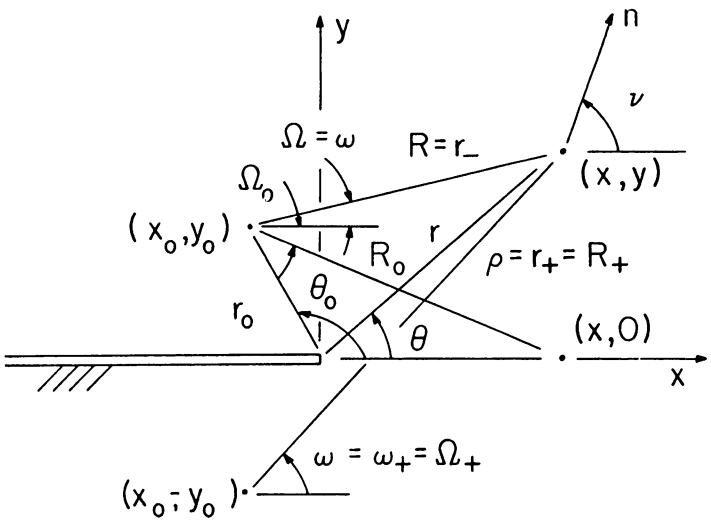

FIG. 3. Illustration of solution parameters.

Some of these observations are illustrated in Fig. 4, where F and dF/dn at the point $(x, y) = (-1.0, 0.5)$ are plotted vs. s for various values of ν and a unit concentrated force imposed at $(x_0, y_0) = (-1.0, 1.0)$. Here (x, y, x_0, y_0, s) have the same arbitrary units of length. As predicted above, discontinuities in dF/dn are seen at the three signal wavefronts, except for the case $\nu = 90°$. Then, no discontinuity occurs when the B-signal arrives $(s = \Delta)$.

6. Concentrated impulse solution. For this problem, b_F is replaced in (2.1) by the impulse representation

$$b_I = \delta(x - x_0)\delta(y - y_0)\delta(s), \quad s = \tau - \tau_0. \tag{6.1}$$

The solution $I(x, y, x_0, y_0, s)$ then obviously follows as the derivative w.r.t s of the concentrated force solution F. That is, one need only replace F in (5.1) and (5.2) with I and redefine the signal terms as

$$A = k_r Q(s, R_+), \quad A_n = k_r R_+ Q^3(s, R_+)\frac{dR_+}{dn}, \quad Q(u, v) = \frac{v}{u}P(u, v), \tag{6.2}$$

$$2B_1 = Q(s, \rho) - Q(s, R), 2B_{1_n} = \rho Q^3(s, \rho)\frac{d\rho}{dn} - RQ^3(s, R)\frac{dR}{dn}, \tag{6.3}$$

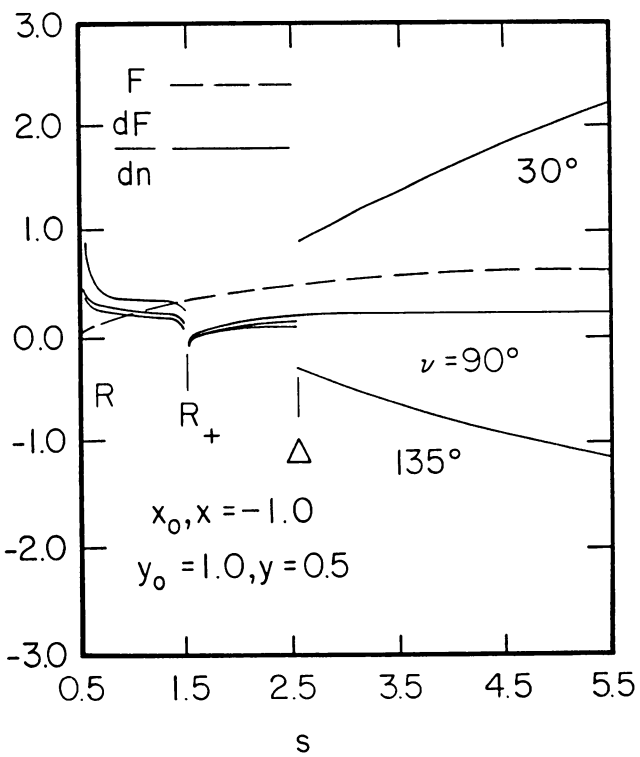

FIG. 4. F, dF/dn vs. s.

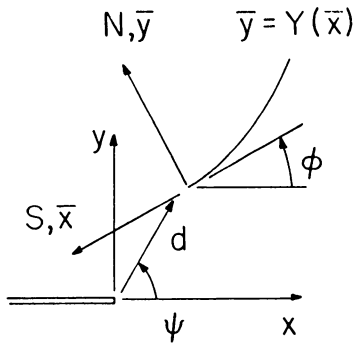

(a)

FIG. 5*a*. Screw dislocation in equilibrium near crack.

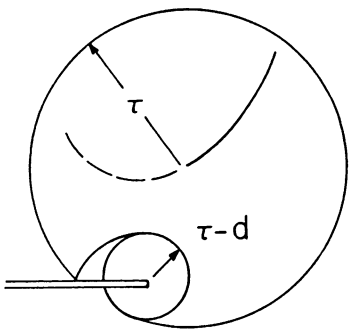

(b)

FIG. 5*b*. Wavefront pattern for dislocation motion.

$$4\pi B_2 = \frac{y_0}{r_0 + x_0}\frac{1}{C}\cos\Phi, \tag{6.4a}$$

$$8\pi B_{2n} = \frac{-y_0}{r_0 + x_0}\frac{1}{C^3}\left[r_+\cos(\phi - \omega_+ - 3\Phi) + r_-\cos(\omega_- - \phi - 3\Phi)\right], \tag{6.4b}$$

$$G = Q(s, R), \qquad G_n = RQ^3(s, R)\frac{dR}{dn}, \tag{6.5}$$

where $(C, \Phi, \omega_\pm, r_\pm)$ are evaluated at $s - r_0$. Eqs. (6.2)–(6.5) show clearly that the signals comprising I and dI/dn are in general not continuous at their respective wavefronts.

7. A Green's function application. As often defined [7], the driving function in a transient Green's function is impulsive in time. Thus, the solution I would be the cracked plane Green's function. However, for the application chosen here, the solution F is seen to be also effective in this role.

Consider the unbounded plane in Fig. 5a containing a semi-infinite crack and a screw dislocation. The dislocation is a unit anti-plane displacement discontinuity along the prescribed path defined by the Cartesian coordinates $\bar{y} = Y(\bar{x})$ or the path coordinates $N = 0$, $S < 0$. For convenience, the coordinate directions $(\bar{x}, S)$ and $(\bar{y}, N)$ coincide at the dislocation edge. The path length parameter S can then be defined as

$$S = \int_0^{\bar{x}} \sqrt{1 + (Y')^2}\, du \tag{7.1}$$

where $(\,)'$ denotes differentiation w.r.t. the argument. The path function $Y(\bar{x})$ is continuous and piecewise smooth. However, it is not required that the inverse $\bar{x} = X(S)$ of (7.1) be single valued. If ϕ is the path slope at the dislocation edge w.r.t. the crack edge-centered Cartesian system (x, y), and (d, ψ) are the polar coordinates of the dislocation edge w.r.t. the crack, then

$$x = -\bar{x}\cos\phi - \bar{y}\sin\phi + d\cos\psi, \qquad y = -\bar{x}\sin\phi + \bar{y}\cos\phi + d\sin\psi. \tag{7.2}$$

For $\tau < 0$ the dislocation and crack are in equilibrium. For $\tau > 0$ the dislocation extends along the path $\bar{y} = Y(\bar{x})$ so that its edge is located at $N = 0$, $S = D(\tau)$. The prescribed function D is continuous, where $D(0) = 0$, $0 \leqslant D \leqslant 1$. The latter inequality precludes supersonic dislocation motion, but is not critical to solving the problem. The wave pattern resulting from the dislocation motion is illustrated in Fig. 5b.

This problem has implications in the dynamic study of damage and plastic zones near crack edges [11]. It was treated in [5] by considering the super-position-related problem defined by subtracting the equilibrium solution from the complete field:

$$\nabla^2 w - \ddot{w} + \frac{1}{\mu}(b - b_0) = 0, \qquad \frac{\partial w}{\partial y} = 0\,(y = 0, x < 0), \quad w \equiv 0\,(\tau < 0). \tag{7.3}$$

Here $w(x, y, \tau)$ is the anti-plane displacement, μ is the elastic shear modulus, and (b, b_0) are, respectively, the Burridge–Knopoff [12] body force representation of the screw dislocation and its equilibrium ($\tau < 0$) value, where

$$b = \mu H[D(\tau) - S]\delta'(N), \quad b_0 = \mu H(-S)\delta'(N). \tag{7.4}$$

In [5] eqs. (7.3) and (7.4) were attacked by the same approach used here to obtain F_c. However, only the crack edge stress field was derived. To obtain w, integrals corresponding to (3.1) and (3.2) must be evaluated, a process which can prove quite difficult. To obtain w, therefore, we employ F.

The variable τ is replaced with τ_0 in (7.3) and (7.4) and the combination $F\nabla^2 w - w\nabla^2 F$ is integrated over the entire xy-plane χ and the region $0 < \tau_0 < \tau$. By using Green's identity and the sifting property of the Dirac function, it is then easily shown that

$$\int_0^\tau w(x_0, y_0, t)\, dt = \frac{1}{\mu}\int_0^\tau \iint_\chi (b - b_0) F(x, y, x_0, y_0, \tau - t)\, dx\, dy\, dt, \tag{7.5}$$

where t is the dummy variable representing τ_0-integration. The functional dependence of F is written explicitly for convenience, while it is understood from (7.4) that (b, b_0) are functions of (x, y, t). Differentiation of (7.5) w.r.t τ, substitution of (7.4), recognition that $\partial F/\partial\tau = -\partial F/\partial t$ while (S, N) form an orthogonal coordinate system in the xy-plane, and integration by parts gives, upon using the sifting property of the Dirac function, the final result

$$w(x_0, y_0, \tau) = -\int_0^\tau \dot{D}(t)\frac{dF}{dN}(\hat{x}, \hat{y}, x_0, y_0, \tau - t)\, dt, \tag{7.6}$$

$$\hat{x} = -X(t)\cos\phi - Y(t)\sin\phi + d\cos\psi, \tag{7.7a}$$

$$\hat{y} = -X(t)\sin\phi + Y(t)\cos\phi + d\sin\psi. \tag{7.7b}$$

The expression for dF/dN in (7.6) follows from (5.2) by replacing n with N, τ_0 with t and (x, y) with $(\hat{x}, \hat{y})$. The Heaviside function arguments in (5.2) then define the actual t-integration limits in (7.6). For subsonic dislocation motion ($D < 1$), however, these limits are always contained in the interval $(0, \tau)$, cf. [5, 13].

Eq. (7.6) shows that the displacement w at a given (x_0, y_0, τ) depends on the history of the product of the dislocation edge speed and the normal derivative of the concentrated force solution w.r.t. the dislocation path at the dislocation edge position. The t-integration

implies that finite discontinuities and integrable singularities in these quantities may not drastically affect the behavior of w.

8. Discussion. The foregoing analysis produced solutions to the transient dynamic problems of an anti-plane concentrated force and impulse imposed near a semi-infinite crack in an unbounded plane. The solutions were obtained in closed form, and showed the component wave signals, and their wavefront behavior.

The solutions were obtained as candidates for use as cracked plane Green's functions in the numerical solution of transient dynamic problems of crack interaction with material boundaries, voids, inclusions or dislocation. The actual application of the present results in this context is currently underway. However, for purposes of illustration, the concentrated force solution was used here to derive the complete solution for a screw dislocation moving arbitrarily both in terms of path and speed near a semi-infinite crack in an unbounded plane.

Acknowledgment. This work was supported by NSF Grant MEA 8319605.

References

[1] J. W. Rudnicki, "Fracture mechanics applied to the earth's crust," in *Annual Review of Earth Planetary Science*, pp. 489–525 (1980)

[2] J. D. Achenbach, A. K. Gautesen, and H. McMaken, *Ray methods for elastic waves in solids—with applications to scattering by cracks*, Pitman, London (1982)

[3] J. D. Achenbach, A. K. Gautesen, and H. McMaken, "Diffraction of elastic waves by cracks-analytical results," in *Elastic Waves and Non-destructive Testing of Materials*, AMD-Vol. 29 (Pao, Y. H., ed.) ASME, New York (1978)

[4] L. M. Brock, *The dynamic 2D analysis of a concentrated force near a semi-infinite crack*, Quart. Appl. Math. **43**, 201–210 (1985)

[5] L. M. Brock, *The dynamic stress intensity factor due to arbitrary screw dislocation motion*, J. Appl. Mech. **50** 383–389 (1983)

[6] I. N. Sneddon, *The use of integral transforms*, McGraw-Hill, New York (1972)

[7] G. F. Carrier and C. E. Pearson, *Partial differential equations*, Academic Press, New York (1976)

[8] B. V. Kostrov, *Unsteady propagation of longitudinal shear cracks*, Prikladnaya Matemi Mekhanika **30** (English translation), 1241–1248 (1966)

[9] J. D. Achenbach, *Extension of a crack by a shear wave*, Zeitschrift für angewandte Mathematik und Physik **21**, 887–900 (1970)

[10] B. O. Pierce and R. M. Foster, *A short table of integrals* (4th ed.), Ginn and Blaisdell, Waltham, MA (1957)

[11] B. A. Bilby and J. D. Eshelby, *Dislocations and the theory of fracture*, in Fracture, Vol. 1, Chapter 2 (H. Liebowitz, ed.) Academic Press, New York (1968)

[12] R. Burridge and L. Knopoff, *Body force equivalents for seismic dislocations*, Bulletin of the Seismological Society of America **54**, 1875–1888 (1964)

[13] L. M. Brock, *The dynamic stress intensity factor for a crack due to arbitrary rectilinear screw dislocation motion*, Journal of Elasticity **13**, 429–439 (1983)